

Collisional relaxation of two-dimensional self-gravitating systems

B. Marcos*

Laboratoire J.-A. Dieudonné, UMR 6621,
Université de Nice — Sophia Antipolis,
Parc Valrose 06108 Nice Cedex 02, France

Systems with long range interactions present generically the formation of quasi-stationary long-lived non-equilibrium states. These states relax to Boltzmann equilibrium following a dynamics which is not well understood. In this paper we study this process in two-dimensional inhomogeneous self-gravitating systems. Using the Chandrasekhar – or local – approximation we write a simple approximate kinetic equation for the relaxation process, obtaining a Fokker – Planck equation for the velocity distribution with explicit analytical diffusion coefficients. Performing molecular dynamics simulations and comparing them with the evolution predicted by the Fokker – Planck equation, we observe a good agreement with the model for all the duration of the relaxation, from the formation of the quasi-stationary state to thermal equilibrium. We observe however an overestimate or underestimate of the relaxation rate of the particles with the slower or larger velocities respectively. It is due to systematic errors in estimating the velocities of the particles at the moment of the collisions, inherent to the Chandrasekhar approximation when applied to inhomogeneous systems. Theory and simulations give a scaling of the relaxation time proportional to the number of particles in the system.

PACS numbers: 04.40.-b, 05.70.Ln, 05.70.-a

I. INTRODUCTION

Systems of particles with long range interactions are those which inter-particle potential at large separation decays slower than the dimension d of space, i.e., $v(r \rightarrow \infty) \sim 1/r^\gamma$ with $\gamma < d$. There are many examples in nature, such as self-gravitating systems in the cosmological and astrophysical context (the large structure of the universe, galaxies, etc), interaction between vortices in two-dimensional hydrodynamics, cold classical atoms or capillary interactions between colloids or granular media (for a review see e.g. [1]). These kinds of systems present very particular properties in thermal equilibrium, such that negative micro-canonical specific heat or inequivalence of statistical ensembles. Their dynamics is also peculiar compared to short range systems: in a first stage there is the generic formation in a few characteristic times τ_{dyn} of a long-lived non-equilibrium state — during the so-called *violent relaxation* process. A typical example of such quasi-stationary states (hereafter QSS) are galaxies or young globular clusters. Then, a comparatively very slow relaxation to thermodynamical equilibrium occurs — called *collisional relaxation* — in a timescale of order $\tau_{coll} \sim N^\delta \tau_{dyn}$, where N is the number of particles and $\delta \geq 1$ depends on the system studied.

The mechanism of collisional relaxation is still not well understood. In the context of gravitational systems, Chandrasekhar found theoretically, in a seminal work [2], an estimate of the relaxation time for gravitational systems in three dimensions. He considered an homogeneous system and computed the change in velocity due

to successive independent collisions¹ of a test particle in a stationary macroscopic configuration. Because of the hypothesis of homogeneity there is no macroscopic scale in the system, which led to an ongoing controversy about the value of the maximal impact parameter of the collisions and in particular how it should scale with N [3–6]. Following this, several studies considered collective effects (e.g. [7]), but still in homogeneous configurations. An explicit theoretical description of the collisional relaxation in inhomogeneous systems is technically much more difficult to derive, being necessary the use of action-angle variables. This description is still lacking, despite recent progress in this direction [8, 9], for a recent review see e.g. [10].

The collisional relaxation has also been studied numerically, for a wide variety of systems. For one-dimensional gravity, a scaling of $\tau_{coll} \sim N\tau_{dyn}$ has been measured for the full relaxation process [11], and in the Hamiltonian Mean Field model the scaling has been found to be dependent on the initial condition: $\tau_{coll} \sim N\tau_{dyn}$ [12], $\tau_{coll} \sim N^{1.7}\tau_{dyn}$ [12] or $\tau_{coll} \sim \exp(N)\tau_{dyn}$ [13]. For dimensions larger than $d = 1$, the relaxation has been estimated studying — for numerical reasons — only its early stage, i.e., for times in which the QSS is weakly perturbed (see e.g. [14, 15]), or performing simulations with a simplified dynamics. For gravity in two-dimensions, in simulations performed imposing radial symmetry, it has been observed $\tau_{coll} \sim N^{1.35}\tau_{dyn}$ [16]. In $d = 3$ dimensions, the Chandrasekhar scaling $\tau_{coll} \sim N/\ln N\tau_{dyn}$ has been verified for gravity (e.g. [4, 14, 17]) and for power-

¹ We will use here, as in the astrophysical literature, the term “collisions”. In the general context of long-range systems it would be more appropriate to call them “finite N effects”.

*Electronic address: bruno.marcos@unice.fr

law potential $u(r) = 1/r^\gamma$, for which has been found $\tau_{coll} \sim N\tau_{dyn}$ if $\gamma < 2$, see [15, 17].

In this paper, we study the collisional relaxation of a self-gravitating system in $d = 2$ dimensions. The interacting potential — solution of the Poisson equation in $d = 2$ dimensions — is $u(r) = g \ln(r)$, where g is the coupling constant. It is an attractive model because it presents the same mechanism of collisions as in $d = 3$ (which is not the case for models in $d = 1$), the system is self-confined (it is not necessary to confine it artificially in a box), thermal equilibrium properties are easily calculated and numerical simulations are easier to perform than in $d = 3$. Moreover, as mentioned above, it was found in [16], using simulations imposing the radial symmetry (particles conserve their initial angular momentum), that the collisional relaxation scales with the number of particles in the unexpected manner $\tau_{coll} \sim N^{1.35}\tau_{dyn}$. In the way in which these simulations have been performed the actual model is quasi one-dimensional, and this result may be in some connection with the striking relaxation time for the HMF model, in which for some initial conditions it has been found to scale as $\tau_{coll} \sim N^{1.7}\tau_{dyn}$.

Another question that will be addressed in this paper is the fact that it has been observed that the Chandrasekhar approximation — or *local approximation* — gives good estimation of the relaxation time not only in homogeneous systems but also in non-homogeneous configurations (see [4–6, 15]), and in particular how it scales (in a non-trivial way) with the number of particles N and the minimal impact parameter [15]. This suggests the possibility to describe, in a good approximation, the whole collisional relaxation process using this approximation (see e.g. [10]), in which the system is treated as locally homogeneous.

This paper is organized as follows. In the Sect. II, we show that, if the QSS which is collisionally relaxing is approximately homogeneous in its center — as it is for many initial conditions for gravitational system in $d = 2$ and $d = 3$ — then treating the system as homogeneous (but finite) is a reasonable approximation. Then, we compute the diffusion coefficients and, neglecting collective effects, we write a Fokker – Planck equation which describes the evolution of the system. In Sect. III, we report simulations using molecular dynamics of the relaxation of the system, for the whole time range between the QSS and the final thermal equilibrium, for two different initial conditions and different number of particles. We will see, that despite the many approximations, the evolution of the velocity pdf is reasonably well described by the theory for intermediate values of the velocity. In Sect. IV will discuss the validity of the Chandrasekhar approximation. In Sect. V we present the conclusions of this study and further perspectives.

II. THEORETICAL DESCRIPTION

We model the generic evolution of the system using the Boltzmann equation for the one point probability density function $f(\mathbf{r}, \mathbf{v}, t)$. We can write it formally as

$$\frac{\partial f}{\partial t} + \mathbf{v} \cdot \frac{\partial f}{\partial \mathbf{r}} + \mathbf{F}[f] \cdot \frac{\partial f}{\partial \mathbf{v}} = \Gamma_c[f], \quad (1)$$

where $\Gamma_c[f]$ is the collision operator. During the relaxation process, the system reaches first a QSS and then evolves (comparatively slowly) through an infinity sequence of QSS, in which

$$\mathbf{v} \cdot \frac{\partial f}{\partial \mathbf{r}} + \mathbf{F}[f] \cdot \frac{\partial f}{\partial \mathbf{v}} = 0. \quad (2)$$

To make Eq. (1) tractable analytically, we will assume that Eq. (2) holds for all times, which implies not taking collective effects into account.

We will focus in this paper on the evolution of the velocity pdf

$$s(\mathbf{v}, t) = \int d^2r f(\mathbf{r}, \mathbf{v}, t). \quad (3)$$

We integrate Eq. (1) over the positions, obtaining, in the approximation (2)

$$\frac{\partial s}{\partial t} = \int d^2r \Gamma_c[f]. \quad (4)$$

In the same manner as in the most studied $d = 3$ case, the relaxation is dominated by *weak collisions* (see e.g. [18]), i.e., the ones for which the trajectories of the particles are weakly perturbed. Moreover, it has been shown that, for times larger than one orbital period, the force correlation function decays rapidly (e.g. as $\sim 1/t^5$ for gravity in $d = 3$ [19]). We may then consider that collisions are independent and the use of a Fokker-Planck approximation of Eq. (4) is therefore justified (see e.g. [10, 20]), which can be written as

$$\frac{\partial s(\mathbf{v}, t)}{\partial t} = \frac{\partial}{\partial v_i} [D_{v_i} s(\mathbf{v}, t)] + \frac{1}{2} \frac{\partial^2}{\partial v_i \partial v_j} [D_{v_i v_j} s(\mathbf{v}, t)], \quad (5)$$

where the diffusion coefficients are defined as average change of the velocity of the particles per unit of time, i.e.,

$$D_{v_i}(\mathbf{v}) = \frac{\langle \Delta v_i \rangle}{\Delta t} \quad (6a)$$

$$D_{v_i v_j}(\mathbf{v}) = \frac{\langle \Delta v_i \Delta v_j \rangle}{\Delta t}. \quad (6b)$$

In Eqs. (5) and (6) we have assumed that the diffusion coefficients are a well defined quantity to describe the relaxation process in an inhomogeneous system. We will see in what follows to what extent it is a good approximation.

The strategy to compute the diffusion coefficients is the following: because collisional relaxation is dominated by weak collisions, i.e., by the ones in which the trajectory of the particles are weakly perturbed (see e.g. [18]), the diffusion coefficients (6) can be calculated computing changes in velocity of the particles considering that they are evolving on their unperturbed orbits (i.e. the ones which corresponds to the mean field $N \rightarrow \infty$ limit). In Subsect. IIA we will then first estimate the mean potential in which the particles are evolving, in Subsect. IIB we will then compute the change in velocity due to one collision and finally in Subsect. IIC we will compute the diffusion coefficients themselves.

A. Mean field potential

We are going to assume that in the region in which particles are collisionally relaxing the density pdf is homogeneous. This distribution generates a harmonic gravitational field. We will see in our simulations (see Sect. III) that it is a very good approximation. Moreover, this is also true for the thermal equilibrium state, which is the final state the system will reach. At thermal equilibrium the potential generated by the QSS (see e.g. [16])

$$\Psi(r) = \frac{gN}{2} \ln(\lambda^2 + r^2) \quad (7)$$

where λ is a constant which depends on the total energy of the system². For $r \lesssim \lambda$ (which corresponds to a scale in which are included half of the particles), the potential is harmonic, i.e.,

$$\Psi(r) \simeq gN \ln \lambda + \omega^2 r^2, \quad (8)$$

where

$$\omega^2 = \frac{gN}{2\lambda^2}. \quad (9)$$

Under the hypothesis that the potential has the form (8), the trajectories of the particles in the central region of the system (where collisional relaxation occurs) can be then well approximated with ellipses. The relative motion of two particles is also therefore an ellipse which can be written as

$$\mathbf{r}(t) = x_0 \sin(\omega t) \hat{x} + y_0 \cos(\omega t) \hat{y}, \quad (10)$$

as it has been sketched in Fig. 1. We expect that the hypothesis (8) is relatively general: it has been shown numerically in $d = 3$ that, for a wide set of initial conditions, the QSS present also a central homogeneous region which decays rapidly to zero at larger scales [21].

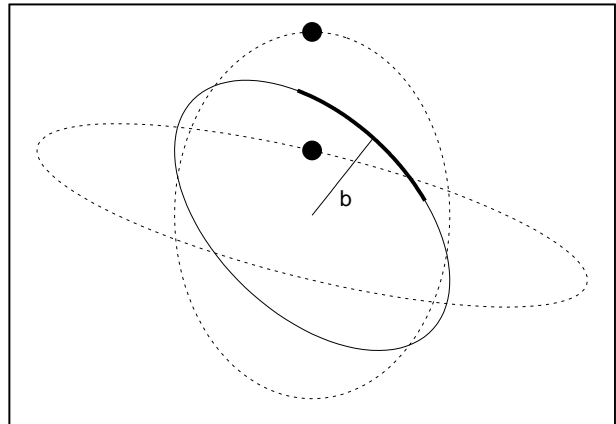


FIG. 1: Sketch of the orbits (dotted curves) of two “colliding” particles (which are plotted at the same arbitrary time). The plain curve represents their relative trajectory, and the thick portion (of length $\sim 2b$) the part of the trajectory in which $|\Delta \mathbf{V}_\perp|$ changes significantly (see text).

B. Computation of the change of velocity due to one “collision”

In the context of long range systems, we define a “collision” between two particles as the process in which they cross each other in half an orbital period (one crossing of the system). Assuming that the relative orbits have the form of Eq. (10) we can compute the change in relative velocity in the \hat{y} direction of two crossing particles by integrating the gravitational acceleration $\mathbf{F}(t)/m$ projected in the \hat{y} direction over the duration of a collision:

$$\begin{aligned} |\Delta \mathbf{V}_y| &= 2g \int_0^{\frac{\pi}{2\omega}} \frac{\mathbf{F}(t) \cdot \hat{y}}{m} dt \\ &\simeq 2g \int_0^{\frac{\pi}{2\omega}} \frac{y_0 \cos(\omega t) dt}{x_0^2 \sin^2(\omega t) + y_0^2 \cos^2(\omega t)} \\ &= 2g \frac{\arctan \left[\sqrt{\frac{x_0^2}{y_0^2} - 1} \right]}{w \sqrt{x_0^2 - y_0^2}}. \end{aligned} \quad (11)$$

From geometrical arguments, it is possible to see that most of the orbits will have large ellipticity. For example, in our simulations we find $y_0/x_0 \approx 0.1$ on average (see Sect. IV). If we choose the axis in order $y_0 < x_0$, then, if the condition

$$y_0 \ll x_0, \quad (12)$$

holds, Eq. (11) can be well approximated by

$$|\Delta \mathbf{V}_y| = \frac{g\pi}{\omega x_0} \left(1 + \mathcal{O} \left(\frac{y_0}{x_0} \right) \right). \quad (13)$$

In Fig. 2 we show how the approximation (13) becomes better increasing the ellipticity x_0/y_0 . For example, a

² The $N \rightarrow \infty$ limit is taken in such a way that $g \propto N^{-1}$, which is equivalent to keep the dynamical time of the system invariant changing N , see Eq. (24). We keep here the dependence on N to have an explicit dependence on τ_{dyn} in our equations.

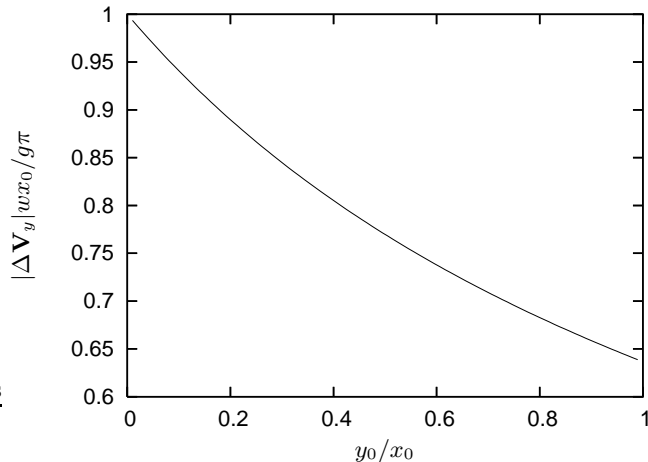


FIG. 2: Continuous line: change in the relative velocity in the y direction $|\Delta \mathbf{V}_y|$ Eq. (11) normalized by its asymptotic value (13) as a function of the ellipticity y_0/x_0 .

maximal relative error of 35% is made for $x_0/y_0 = 1$ decreasing rapidly to an error of 6% when $x_0/y_0 = 0.1$. From Eq. (11) it is possible to see that the “collision” is localized in space and time: as the integral converges rapidly, an excellent approximation of (11) — with the condition (12) — consists in taking as upper cutoff of the integral $\omega t \simeq y_0/x_0$. This means that most of the change of velocity occurs during the interval of time $\Delta t \simeq \omega^{-1}y_0/x_0$ centered around $t = 0$ in our parametrization (10), in a region of length $\sim 2y_0$.

In order to compute simply averages over the velocity pdf in what follows, it is useful to have an expression of the change of velocity as a function of the velocity of the particle itself. In the same approximation (12) we have

$$|\mathbf{V}(t=0)| \equiv V \simeq \omega x_0 \left(1 + \mathcal{O}\left(\frac{y_0}{x_0}\right) \right). \quad (14)$$

Then

$$|\Delta \mathbf{V}_y| \equiv |\Delta \mathbf{V}_\perp| \simeq \frac{g\pi}{V}, \quad (15)$$

where V is the relative velocity at the distance of closest approach. We use the notation \mathbf{V}_\perp because, in this approximation, $\Delta \mathbf{V}_y$ corresponds to the change of velocity in the perpendicular direction of the velocity of the particle. This result is the one obtained by Chandrasekhar adapted to self-gravitating systems in $d = 2$ dimensions. We will discuss the implications and limitations of this approach in Sect. IV.

It is possible to compute the change in the relative parallel velocity using that, in a weak collision, V does not change during the collision. Then:

$$|\Delta \mathbf{V}_\perp| = V \sin \theta \quad (16a)$$

$$|\Delta \mathbf{V}_\parallel| = V(1 - \cos \theta), \quad (16b)$$

where θ is the angle of deflection. In the weak collision approximation $\theta \ll 1$ and thus we have $\sin \theta \simeq \theta$ and $\cos \theta \simeq 1 - \theta^2/2$ and then

$$|\Delta \mathbf{V}_\parallel| = \frac{|\Delta \mathbf{V}_\perp|^2}{2V}. \quad (17)$$

Taking into account that particle masses are equal we obtain for the change in velocity of a particle, using Eqs. (15) and (17),

$$|\Delta \mathbf{v}_\perp| \simeq \frac{\pi g}{2V} \quad (18a)$$

$$|\Delta \mathbf{v}_\parallel| \simeq \frac{\pi^2 g^2}{4V^3}. \quad (18b)$$

C. Computation of the diffusion coefficients

We compute the diffusion coefficients using the standard method used in $d = 3$ in the local approximation. As the spatial density pdf is approximately constant up to a scale r^* in radial coordinates (see discussion above and numerical simulations of Sect. III), we can therefore estimate the number η of collisions of a particle in an time interval Δt , on average, as

$$\eta \simeq \frac{2NV\Delta t}{\pi r^*}; \quad (19)$$

the factor $\pi r^*/2$ is the average height of a circle of radius r^* . We are going now to average over the velocity pdf. We will do a somewhat uncontrolled approximation here because Eq. (15) gives the change of relative velocity *at the point of closest approach*. It is not possible to compute exactly this quantity from the velocity pdf because the change in velocity of a particle does not depend on its velocity (as in the homogeneous case) but in the orbit to which it behaves, i.e., in the particular values of x_0 and y_0 corresponding to the particle. To go further, however, we will assume that it is possible to average over the velocity pdf $s(v)$. Introducing, as in the $d = 3$ case, the Rosenbluth potential [22]

$$q(v) = \int d^2 v' \frac{s(v')}{|\mathbf{v} - \mathbf{v}'|} \quad (20a)$$

$$p(v) = \int d^2 v' s(v') |\mathbf{v} - \mathbf{v}'|, \quad (20b)$$

and assuming that the velocity pdf is isotropic, we obtain, keeping only terms of $\mathcal{O}(g^2)$ (see App. A):

$$D_{v_i}(v) = \frac{\langle \Delta v_i \rangle}{\Delta t} = C \frac{\partial q(v)}{\partial v_i} \quad (21a)$$

$$D_{v_i v_j}(v) = \frac{\langle \Delta v_i \Delta v_j \rangle}{\Delta t} = C \frac{\partial^2 p(v)}{\partial v_i \partial v_j},$$

where

$$C = \frac{\pi g^2 N}{2r^*}. \quad (22)$$

As the succession of QSS have an approximate polar symmetry, it is then useful to write Eq. (5) in polar coordinates. Considering that the Rosenbluth potentials are isotropic, we get using Eq.(A7)

$$\frac{\partial \tilde{s}}{\partial t} = C \left\{ -\frac{\partial}{\partial v} \left[\left(q'(v) + \frac{p'(v)}{2v^2} \right) \tilde{s} \right] + \frac{1}{2} \frac{\partial^2}{\partial v^2} [p''(v)\tilde{s}] \right\}, \quad (23)$$

where $\tilde{s}(v)$ as the velocity pdf in polar coordinates, $v = |\mathbf{v}|$ and the primes denotes derivation with respect to v . It is useful to write Eq. (23) in an adimensional form. We define the our time unit as the dynamical time of the system

$$\tau_{dyn} = \frac{1}{\sqrt{gN}}. \quad (24)$$

We define the velocity units v_* using the virial theorem, which states that, for any stationary state (and hence a QSS), the average velocity square of the particles is constant during the evolution (e.g. [16, 23]):

$$\langle v^2 \rangle = \frac{gN}{2}. \quad (25)$$

It is then natural to take as velocity unit

$$v_* = \sqrt{gN}. \quad (26)$$

Defining the adimensional time and velocities as $\tilde{t} = t/\tau_{dyn}$ and $\tilde{v} = v/v_*$ respectively, we get from Eq. (23)

$$\frac{\partial \tilde{s}}{\partial \tilde{t}} = \hat{C} \left\{ -\frac{\partial}{\partial \tilde{v}} \left[\left(q'(\tilde{v}) + \frac{p'(\tilde{v})}{2\tilde{v}^2} \right) \tilde{s} \right] + \frac{1}{2} \frac{\partial^2}{\partial \tilde{v}^2} [p''(\tilde{v})\tilde{s}] \right\}, \quad (27)$$

where we have defined

$$\hat{C} = C \frac{\tau_{dyn}}{v_*^3} = \frac{\pi}{2Nr_*}. \quad (28)$$

Equation (27) depends on N through \hat{C} , which implies that the relaxation scales as

$$\tau_{coll} \sim N\tau_{dyn}. \quad (29)$$

To compute explicitly the diffusion coefficients we need an explicit form of $\tilde{s}(\tilde{v})$. As discussed above, the velocity pdf at the distance of closest approach is unknown. We will use then the standard approximation to take the equilibrium Maxwell – Boltzmann pdf (see e.g. [10])

$$\tilde{s}_{MB}(\tilde{v}) = 2\tilde{v}v_*\beta \exp(-\beta\tilde{v}^2), \quad (30)$$

with $\beta = 2$ given by Eq. (25). We obtain in this approximation

$$q(\tilde{v}) = e^{-\beta\tilde{v}^2/2} \sqrt{\pi\beta} I_0 \left(\frac{\beta\tilde{v}^2}{2} \right) \quad (31a)$$

$$p(\tilde{v}) = \frac{1}{2} \sqrt{\frac{\pi}{\beta}} e^{-\beta\tilde{v}^2/2} \left[-e^{\beta\tilde{v}^2/2} + (1 + \beta\tilde{v}^2) I_0 \left(\frac{\beta\tilde{v}^2}{2} \right) + \beta\tilde{v}^2 I_1 \left(\frac{\beta\tilde{v}^2}{2} \right) \right], \quad (31b)$$

where $I_n(x)$ is the modified Bessel function of the first kind. It is possible to verify that the equilibrium pdf (30) is a stationary solution of Eq. (27) with the diffusion coefficients given by Eq. (31). Note that we obtain the same result obtained in [24] (see also [25]), in which a different method to compute the diffusion coefficients than Rosenbluth potentials has been used.

III. NUMERICAL SIMULATIONS

We compare the theoretical model with molecular dynamics simulations performed with a modification of the publicly available code GADGET2 [26] to handle the logarithmic interaction. We use a time-step of $2.5 \times 10^{-4}\tau_{dyn}$ in order to ensure a very precise energy conservation, which is better than 10^{-5} for the whole duration of the runs. We performed simulations with initial water-bag conditions with different number of particles in the interval $N = [100, 8000]$ and initial virial ratio $\mu_0 = 1$ and $\mu_0 = 1.7$, where

$$\mu_0 = \frac{v_*}{\sqrt{2\langle v_0^2 \rangle}}, \quad (32)$$

where $\langle v_0^2 \rangle$ is the average of the initial velocity square. The simulations have been performed for times of $5600\tau_{dyn}$ for the systems with the largest N and $7700\tau_{dyn}$ with the smallest one. In order to improve statistics, we average the measured velocity pdf over 100 consecutive snapshots in an interval of $2.5\tau_{dyn}$. The system forms a QSS which is approximately homogeneous in its central region, with a rapid decay of the density at larger scale, as it can be seen in Fig. 3 for both initial conditions. We observe that the one with initial virial ratio $\mu_0 = 1$ gives rise to a compact density pdf whereas the one with initial virial ratio $\mu_0 = 1.7$ to a core halo distribution. In Fig. 4 we plot the potential energy $\Psi(r)$ generated by the density pdf at time $t = 50\tau_{dyn}$ (time in which the system has violently relaxed) and $t = 5600\tau_{dyn}$, corresponding to thermal equilibrium for the $\mu_0 = 1.7$ case (an analogous result is obtained for $\mu_0 = 1.7$). We observe that for the inner part of the system the potential is very well approximated by the potential generated by the system at thermal equilibrium (8). We monitor how the system approaches thermal equilibrium using the parameter

$$\xi(t) = \frac{1}{N^2} \int_0^\infty [s(v, t) - s_{MB}(v)]^2 dv. \quad (33)$$

In order to compare simulations with theory we compute the associated Langevin equation of Eq. (27). Therefore, the change in the velocity is given, following the Ito definition, by

$$d\tilde{v}(\tilde{t}) = \hat{C} \left\{ \left(q'(\tilde{v}) + \frac{p'(\tilde{v})}{2\tilde{v}^2} \right) d\tilde{t} + \sqrt{p''(\tilde{v})} dW \right\}, \quad (34)$$

where dW is a Gaussian stochastic variable delta correlated in time with variance unity. We choose as initial

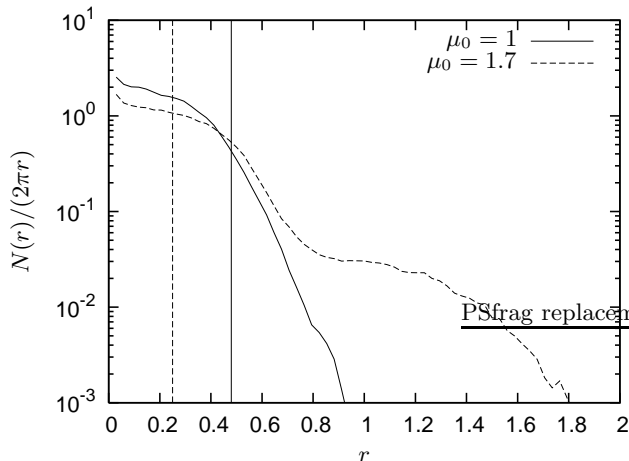


FIG. 3: Density pdf in the QSS at $t = 50\tau_{dyn}$ for both initial condition. The vertical curves (of the same type of their corresponding density profile) are the values of r^* used in (19) in order to obtain the measured relaxation rate in the simulations.

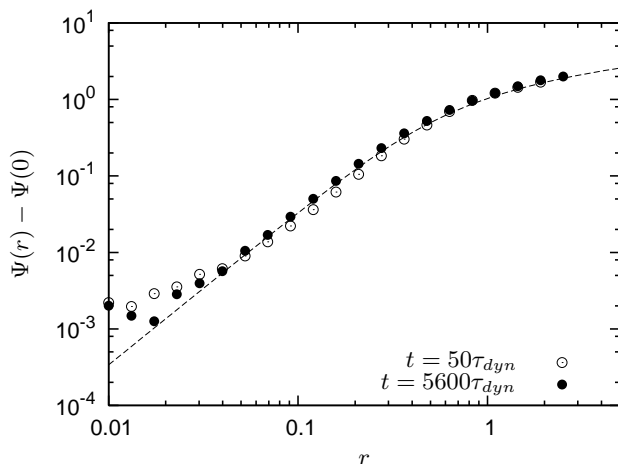


FIG. 4: Potential of the particles in function of their radial distance for the simulation with $\mu_0 = 1.7$, at $t = 50\tau_{dyn}$ and $t = 5600\tau_{dyn}$. The dashed line is the potential of the distribution at thermal equilibrium (7).

condition a configuration of the numerical simulation at $t = 50\tau_{dyn}$ (time in which the system has violently relaxed) and then we compare the evolution predicted by the Langevin equation and the one of the full numerical simulation. We integrate Eq. (34) by a simple Euler procedure. In Fig. 5 we show the evolution of $\xi(t)$, where the time axis has been rescaled by a factor N , which indicates a scaling of the relaxation time as $\tau_{coll} \sim N\tau_{dyn}$. For clarity, between all the simulations with different numbers of particles performed we plot three of them. The part of the curve which flattens corresponds to thermal equilibrium, which is attained first as N decreases. The

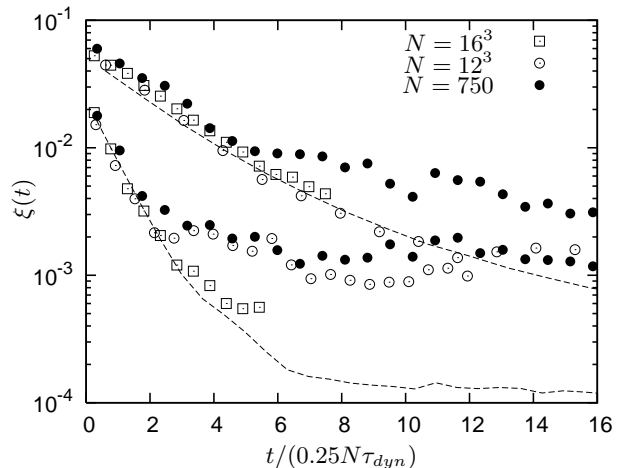


FIG. 5: Upper curves: initial condition with $\mu_0 = 1$. Lower curves: initial conditions with $\mu_0 = 1.7$. Points: evolution of the crossover parameter $\xi(t)$ measured in the molecular dynamics simulations for the two different initial condition $\mu_0 = 1$ and $\mu_0 = 1.7$. Lines: theoretical prediction calculated using Eq. (34) for each case (see text).

matching between the curves corresponding to different N is very good in the region out of equilibrium, as it has been illustrated for $N = 750$, $N = 12^3$ and $N = 16^3$, which confirm the prediction of Eq. (27) for the scaling of the relaxation. The dashed curves corresponds to the theoretical prediction given by Eq. (34) with $r^* = 0.48$ for the simulation with $\mu_0 = 1$ and $r^* = 0.25$ for the simulation with $\mu_0 = 1.7$. These values are, within a factor 2, close to the scale of the falloff in the density pdf; the density decays to half its center value around $r \approx 0.4$ for both set of simulations. We emphasize that the difference in the slopes of the curves is essentially due to the different initial conditions considered for each case rather than in the value of r^* taken: taking indeed the same value of r^* for both initial conditions the two curves appear to be very different. The full simulation curves decay to a lower value at thermal equilibrium because fluctuations appears to be larger in the molecular dynamics simulations than in the Langevin simulation. In Fig. 6 we show the evolution of the full velocity pdf for both the simulation and the theory. The first two rows of the figure corresponds to the case $\mu_0 = 1$ and $\mu_0 = 1.7$ respectively. In the next two rows of the figure we reproduce the same plots but in log-linear scale to appreciate the tails of the distribution. We observe that the model predicts very well the evolution of the velocity pdf for *intermediate* values of the velocities. For low velocities it predicts systematically a relaxation *faster* than the observed in the simulation, whereas for large velocities it predicts systematically a relaxation slower than the one observed in the simulations (in the latter case specially for the $\mu_0 = 1.7$ system). We will discuss this discrepancy in the following section.

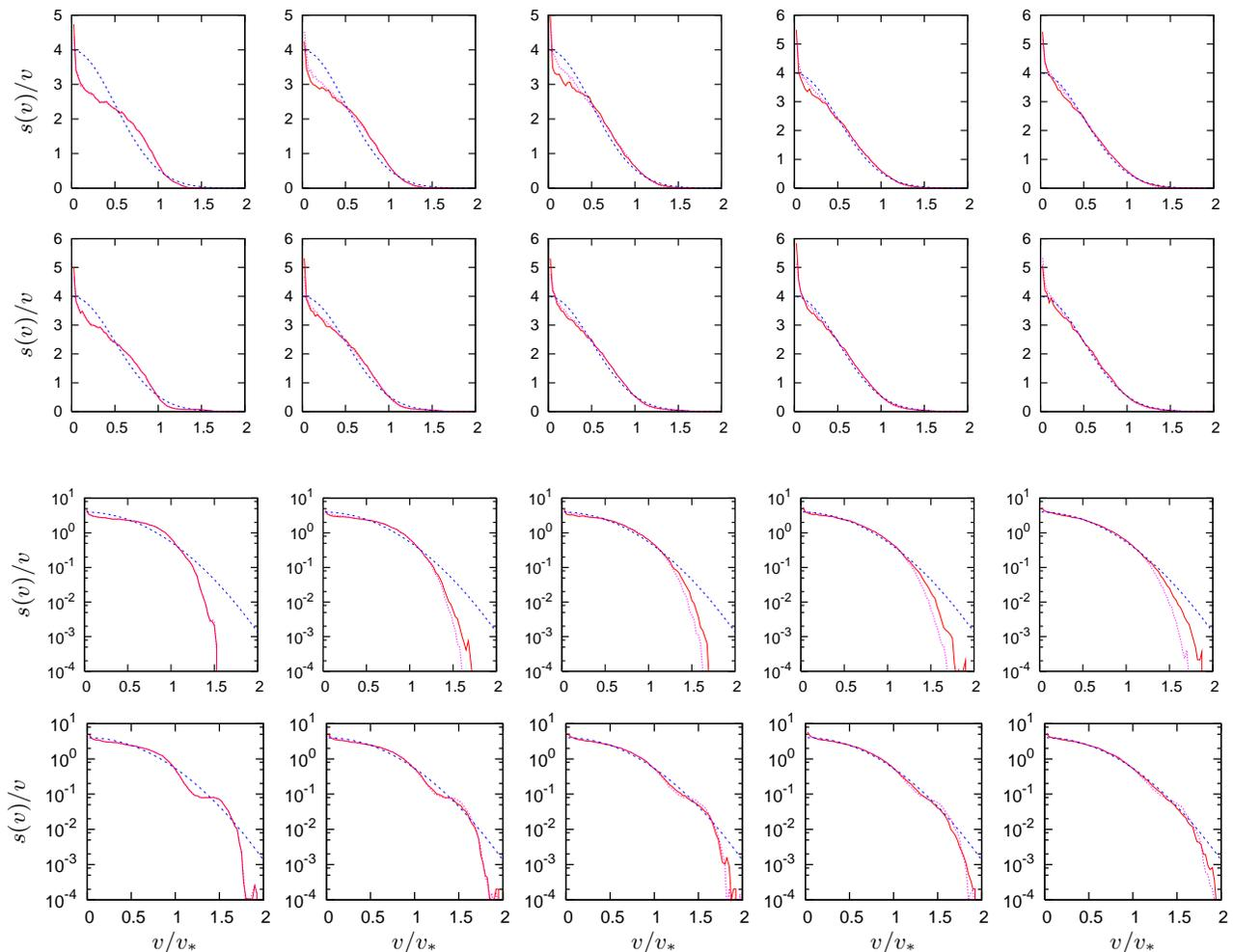


FIG. 6: First row of plots: evolution of the velocity pdf for $\mu_0 = 1$ and times $t = (20, 1550, 3100, 4650, 6200)\tau_{dyn}$. Second row of plots: evolution of the velocity pdf for $\mu_0 = 1.7$ and times $t = (20, 520, 1030, 1550, 2060)\tau_{dyn}$. The second block of plots are exactly the same but in log-linear scale. The plain red curve represents the simulations, the pink dotted one the theoretical prediction and the blue dashed curve the thermal equilibrium pdf (30).

IV. THE VALIDITY OF THE CHANDRASEKHAR APPROXIMATION APPLIED TO INHOMOGENEOUS SYSTEMS

It is possible to show that the result (15) is the same one than the one obtained in the spatial homogeneous case originally treated by Chandrasekhar applied to gravity in $d = 2$. In this study, it was considered rectilinear trajectories with constant relative velocity V (e.g. [18]), in which the distance of closest approach y_0 is the impact factor b . Then

$$|\Delta \mathbf{V}_\perp| \simeq 2 \int_0^\infty \frac{gb}{b^2 + (Vt)^2} dt = \frac{g\pi}{V}. \quad (35)$$

The agreement between the results can be understood for two reasons:

1. trivially, in the limit $y_0/x_0 \rightarrow 0$, the unperturbed trajectories (10) become rectilinear, and

2. an excellent approximation to the integral (35) is obtained taking $t \simeq b/V$ as upper cutoff, i.e., the collision is localized in the same sense than the one discussed for the integral of Eq. (11).

Therefore we can conclude, that when the relative orbits have large ellipticity, the system can be treated as locally homogeneous and Eq. (35) would be a good approximation. We have checked that it is the case in our system, as it can be seen in Fig. 7. In this figure, we measure from the simulations the value of y_0/x_0 for all the possible relative orbits (i.e. $N(N-1)/2$ in total) at $t = 50\tau_{dyn}$. We stress however that, as discussed above, it is not possible to average properly over velocities: the appropriate velocity pdf which must be used in Eqs. (11) and (35) is not the velocity pdf but the *velocity pdf at the moment of the collision*. Having this idea in mind we obtain a very coherent picture to explain the results obtained in Fig. 6:

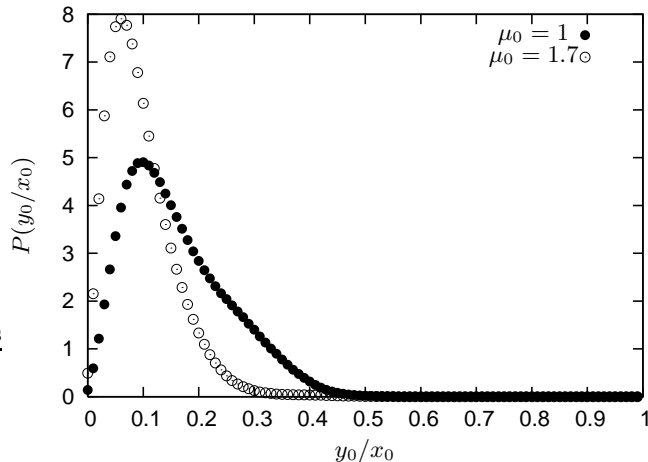


FIG. 7: Distribution of eccentricities $P(y_0/x_0)$ measured at $t = 50\tau_{dyn}$ for both initial conditions.

- Particles with large velocity are very likely to be at the perigee of their orbit, i.e., the portion of the orbit in which the velocity is maximal. Hence, during the successive collisions, it is very probable that they would be in another portion of their orbit, with smaller velocity. Therefore, velocities at the moment of the collisions is systematically overestimated and, using Eq. (13) (or Eq. (31)), the relaxation rate predicted by the Chandrasekhar approximation will be faster than the one which actually happens in the system.
- The opposite occurs for low velocities: particles are more likely to be at the apogee of their orbit. Therefore, the velocity in the moment of the collisions is systematically underestimated, and then, for the same reason than above, the Chandrasekhar approximation predicts a relaxation rate slower than the one which actually occurs.

The arguments presented above apply also in $d = 3$, which may explain why the original Chandrasekhar approach gives a good estimate of the relaxation time in inhomogeneous systems, taking as maximal impact parameter the size of the system (see e.g. [6, 14]). In particular:

- We expect that, in the same way than in the case studied here, the mean field potential would not change too much during the collisional relaxation process, which essentially makes the dynamical time τ_{dyn} invariant.
- It has been shown numerically in $d = 3$ that, for a wide set of initial conditions, the QSS presents also a central homogeneous region which decays rapidly to zero at larger scales [21]. Our hypothesis of Subsect. II A would be therefore fulfilled.

- All the arguments of Subsect. II B would also be true, and in particular the change of velocity due to one collision would have the same properties than Eq. (11), as we will show below.

Because collisions occurs also in a plane, we would have now

$$\begin{aligned}
 |\Delta \mathbf{V}_y| &\simeq 2g \int_0^{\frac{\pi}{2\omega}} \frac{y_0 \cos(\omega t) dt}{(x_0^2 \sin^2(\omega t) + y_0^2 \cos^2(\omega t))^{3/2}} \\
 &= \frac{2g}{\omega x_0 y_0}.
 \end{aligned} \tag{36}$$

In the limit $y_0/x_0 \rightarrow 0$, and using Eq. (14), we get the well-known result of Chandrasekhar [2]:

$$|\Delta V_{\perp}| \simeq \frac{2g}{Vb}. \tag{37}$$

Collisions are then “local”, in the same manner than in the case discussed in the paper, i.e., the change in velocity occurs in a region of space of order of the impact factor. Analogously than in the case treated in the paper it is difficult to estimate the statistics of the relative velocities at the distance of closest approach. However, the dependence of the change in velocity with the impact factor is expected to be an excellent approximation. As Eq. (37) factorizes between a part which depends on the velocity and another one on the impact factor b , even if we do an error computing averages over velocities we would obtain the Coulomb logarithm $\ln(R/b_{min})$ integrating over the allowed impact factors (b_{min} is the minimal impact factor). This explains why the relaxation rate measured in simulations scales with the Coulomb logarithm, as observed in simulations in gravitational systems in $d = 3$ [4–6, 15, 17].

V. DISCUSSION

In this paper we have shown that using a “minimal” model — based on the Chandrasekhar approximation — we can describe well the evolution of the velocity distribution of a gravitational system in $d = 2$, for times from the formation of the QSS to thermal equilibrium. We have derived an explicit kinetic equation neglecting collective effects, in which we slightly adjust a single free parameter r^* . Comparing the evolution of the velocity distribution observed in the simulation and the one calculated with the model, we obtain a good agreement for all times, from the formation of the QSS to thermal equilibrium.

We can conclude, as we anticipated in the Introduction, that the Chandrasekhar (or local) approximation gives a reasonable description of the collisional relaxation in this system. This is due to the fact that many of the relative orbits of the particles which can be well approximated by ellipses which large ellipticity, for which the Chandrasekhar approximation is a good one. However,

a systematic error is made computing the diffusion coefficients, because the velocity of the particles *during the collisions* does not correspond in general to the velocity of the particle at the moment in which we sample the velocity pdf. Because of that, we have shown that we overestimate systematically the relaxation rate of the particles with small velocity and we underestimate systematically the relaxation rate of particles with large velocities.

We have neglected possible resonances of the particles with the mean field potential. We expect that they are not important, because particles have the same mass, which is a very different situation of the decay of a single much massive particle inside a QSS formed by much lighter ones, which can excite resonances (see e.g. [27]). Moreover, the actual potential in which particles are moving is not harmonic but is close to the one of Eq. (7): particles present highly precessing quasi-periodic orbits, which are very unlikely to excite resonances by crossing the system again and again following the same trajectory.

On an other side, we do not observe numerically the scaling $\tau_{coll} \sim N^{1.35} \tau_{dyn}$ observed in [16]. This is due to the fact that they use a simplified dynamics (polar symmetry is imposed along all the run and therefore particles conserve their initial angular momentum) appear not to describe properly the collisional dynamics of the real $d = 2$ system. A possible explanation of this discrepancy is that the model presented in [16] is not truly two-dimensional but quasi one-dimensional. It is known that one-dimensional models as the HMF can present striking scalings of the relaxation time with N , as pointed out in the introduction. Interestingly, however, the same group get, using the same simplified dynamics in $d = 3$, the same scaling $\tau_{coll} \sim N \tau_{dyn}$ observed using full numerical simulations [28]. More investigation should be done to understand this discrepancy.

Some conclusions can be made about the maximal impact parameter which has to be considered in the calculations. In the simulations we do not observe any dependence of r^* — which is directly related with the maximal impact parameters allowed — with the number of particles N . We can conclude then that the maximum impact parameter does not depend on a scale related to the interparticle distance — which scales as $N^{-1/2}$ — but with the size of the system. Moreover, we obtain an actual value of r^* which corresponds to the size of the homogeneous part of the system. This result is in agreement with simulations performed in $d = 3$ dimensions [17] with potential interactions $u(r) \sim 1/r^\gamma$, $\gamma \leq 2$, in which the maximal impact parameter to take in the Chandrasekhar approximation was numerically estimated to be $1/3$ the size of the system.

We can conclude that to obtain a better description of the collisional relaxation, the use of action – angle variables is unavoidable. When performing the calculation of Eq. (11) we are indeed using action – angle variables, the parameters x_0 and y_0 being proportional to the two actions of the system. A complete calculation using canonical perturbation theory is however much more

involved.

Acknowledgments

I am very grateful to M. Joyce and Y. Levin for many discussions which made this work possible. I acknowledge for many useful discussions J. Barré, C. Nardini, R. Pakter, F. Peruani, A. C. Ribeiro Teixeira, T. Teles and D. Vincenzi. I warmly thank M. Courtney for her lecture of a previous version of the paper. Numerical simulations have been performed at the cluster of the SIGAMM hosted at “Observatoire de Côte d’Azur”, Université de Nice – Sophia Antipolis. This work was partly supported by the ANR 09-JCJC-009401 INTERLOP project and the CNPq PDS 158378/2012-1 grant.

Appendix A: Computation of the diffusion coefficients

We define a laboratory Cartesian system of coordinates with unit vectors \hat{e}_i ($i = 1, 2$), and another Cartesian system of coordinates \hat{e}'_i , in which \hat{e}'_1 is in the direction of the initial relative velocity. We have therefore

$$\Delta \mathbf{v} = -|\Delta \mathbf{v}_\parallel| \hat{e}'_1 + |\Delta \mathbf{v}_\perp| \hat{e}'_2 \quad (\text{A1})$$

The projection of the velocity in the \hat{e}_i direction is then

$$\Delta v_i = -|\Delta \mathbf{v}_\parallel| \hat{e}'_1 \cdot \hat{e}_i + |\Delta \mathbf{v}_\perp| \hat{e}'_2 \cdot \hat{e}_i. \quad (\text{A2})$$

Taking into account that, in average, collisions which will give rise to a change of the perpendicular velocity are equally probable in the \hat{e}'_2 direct in and in the direction opposite to it, we can write

$$\Delta v_i = -|\Delta \mathbf{v}_\parallel| \frac{V_i}{V} \quad (\text{A3a})$$

$$\Delta v_i \Delta v_j = |\Delta \mathbf{v}_\perp|^2 \left(\delta_{ij} - \frac{V_i V_j}{V^2} \right), \quad (\text{A3b})$$

where we have kept only the terms of $\mathcal{O}(g^2)$ and used that $\hat{e}'_1 \cdot \hat{e}_i = V_i/V$ and $(\hat{e}'_2 \cdot \hat{e}_i)(\hat{e}'_2 \cdot \hat{e}_j) = \delta_{ij} - V_i V_j/V^2$. The diffusion coefficients are:

$$D_{v_i} = \frac{\langle \Delta v_i \rangle}{\Delta t} = -C \int d^2 v' s(v') \frac{V_i}{V^3} \quad (\text{A4a})$$

$$D_{v_i v_j} = \frac{\langle \Delta v_i v_j \rangle}{\Delta t} = C \int d^2 v' \frac{s(v')}{V} \left(\delta_{ij} - \frac{V_i V_j}{V^2} \right). \quad (\text{A4b})$$

Introducing, as in the $d = 3$ case, the Rosenbluth potential, we can write the diffusion coefficient using Eqs. (19) and (22)

$$D_{v_i}(v) = C \frac{\partial q(v)}{\partial v_i} \quad (\text{A5a})$$

$$D_{v_i v_j}(v) = C \frac{\partial^2 p(v)}{\partial v_i \partial v_j}, \quad (\text{A5b})$$

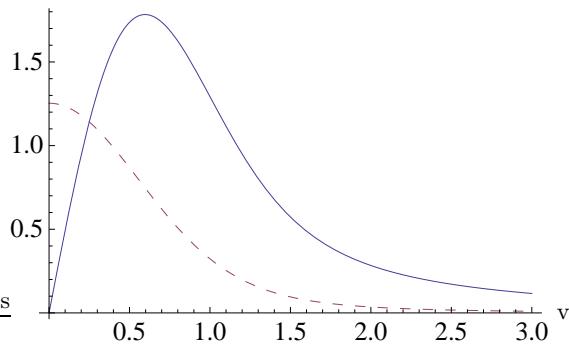


FIG. 8: Plot of $q'(v)$ (straight line) and $p''(v)$ (dashed line) in function of v .

where

$$q(v) = \int d^2v' \frac{s(v')}{|\mathbf{v} - \mathbf{v}'|} \quad (\text{A6a})$$

$$p(v) = \int d^2v' s(v') |\mathbf{v} - \mathbf{v}'|, \quad (\text{A6b})$$

where we have assumed that the velocity pdf is isotropic. Using that the Rosenbluth potentials are isotropic we can simplify Eqs. (A5) using that

$$\frac{\partial q(v)}{\partial v_i} = \frac{v_i}{v} q'(v) \quad (\text{A7a})$$

$$\frac{\partial^2 p(v)}{\partial v_i \partial v_j} = \frac{v_i v_j}{v^2} \left(p''(v) - \frac{p'(v)}{v} \right) + \delta_{ij} \frac{p'(v)}{v}, \quad (\text{A7b})$$

where the prime denotes derivative with respect to v . In Fig. 8 we plot $q'(v)$ and $p''(v)$, which gives of $D_{v_i}(v)$ and $D_{v_i v_j}(v)$ respectively.

-
- [1] A. Campa, T. Dauxois, and S. Ruffo, *Phys. Reports* **480**, 57 (2009), arXiv: 0907.0323.
- [2] S. Chandrasekhar, *Principles of stellar dynamics* (University of Chicago Press, 1942).
- [3] M. Hénon, *Annales d'Astrophysique* **21**, 186 (1958).
- [4] R. T. Farouki and E. E. Salpeter, *Astrophys. J.* **253**, 512 (1982).
- [5] H. Smith, Jr., *Astrophys. J.* **398**, 519 (1992).
- [6] R. T. Farouki and E. E. Salpeter, *Astrophys. J.* **427**, 676 (1994).
- [7] M. D. Weinberg, *Astrophys. J.* **410**, 543 (1993).
- [8] J. Heyvaerts, *Mon. Not. R. Astr. Soc.* **407**, 355 (2010).
- [9] P.-H. Chavanis, *Physica A Statistical Mechanics and its Applications* **391**, 3680 (2012), 1107.1475.
- [10] P.-H. Chavanis, ArXiv e-prints (2012), 1210.5743.
- [11] M. Joyce and T. Worrakitpoonpon, *Journal of Statistical Mechanics: Theory and Experiment* **10**, 12 (2010), 1004.2266.
- [12] Y. Y. Yamaguchi, J. Barré, F. Bouchet, T. Dauxois, and S. Ruffo, *Physica A* **337**, 36 (2004), cond-mat/0312480.
- [13] A. Campa, P.-H. Chavanis, A. Giansanti, and G. Morelli, *Phys. Rev. E* **78**, 040102 (2008), 0807.0324.
- [14] J. Diemand, B. Moore, J. Stadel, and S. Kazantzidis, *Mon. Not. Roy. Astron. Soc.* **348**, 977 (2004).
- [15] A. Gabrielli, M. Joyce, and B. Marcos, *Physical Review Letters* **105**, 210602 (2010), 1004.5119.
- [16] T. N. Teles, Y. Levin, R. Pakter, and F. B. Rizzato, *Journal of Statistical Mechanics: Theory and Experiment* **5**, 7 (2010), 1004.0247.
- [17] B. Marcos, A. Gabrielli, and M. Joyce, in preparation.
- [18] J. Binney and S. Tremaine, *Galactic Dynamics* (Princeton University Press, 2008).
- [19] L. Cohen and A. Ahmad, *Astrophys. J.* **197**, 667 (1975).
- [20] H. Risken, *The Fokker-Planck equation. Methods of solution and applications* (Springer, Berlin, 1989, 2nd ed.).
- [21] F. Roy and J. Perez, *Mon. Not. R. Astr. Soc.* **348**, 62 (2004).
- [22] N. Rostoker and M. N. Rosenbluth, *Physics of Fluids* **3**, 1 (1960).
- [23] P.-H. Chavanis, *Comptes Rendus Physique* **7**, 331 (2006), arXiv:astro-ph/0612086.
- [24] P. H. Chavanis, *European Physical Journal B* **52**, 61 (2006), arXiv:cond-mat/0510078.
- [25] P. H. Chavanis, *European Physical Journal Plus* **127**, 19 (2012), 1112.0772.
- [26] V. Springel, *Mon. Not. R. Astron. Soc.* **364**, 1105 (2005), arXiv:astro-ph/0505010.
- [27] J. I. Read, T. Goerdt, B. Moore, A. P. Pontzen, J. Stadel, and G. Lake, *Mon. Not. Roy. Astron. Soc.* **373**, 1451 (2006), arXiv:astro-ph/0606636.
- [28] Y. Levin, R. Pakter, and F. B. Rizzato, *Phys. Rev.* **E78**, 021130 (2008).